Cancer Letters 442 (2019) 40–52

Contents lists available at ScienceDirect

Cancer Letters

journal homepage: www.elsevier.com/locate/canlet

Original Articles

Diet-induced hepatic steatosis activates Ras to promote hepatocarcinogenesis via CPT1α

An Xu[a,b,1], Bibo Wang[a,c,1], Jing Fu[a,b,1], Wenhao Qin[a], Ting Yu[a,d], Zhishi Yang[a], Qingjun Lu[e], Jingyi Chen[a,b], Yao Chen[a,b,**], Hongyang Wang[a,b,d,*]

[a] International Cooperation Laboratory on Signal Transduction, Eastern Hepatobiliary Surgery Hospital, Second Military Medical University, Shanghai, China
[b] National Center for Liver Cancer, Shanghai, China
[c] Jinling Hospital, School of Medicine, Nanjing University, Nanjing, China
[d] Fuling Central Hospital of Chongqing City, Chongqing, China
[e] State Key Laboratory of Oncogenes and Related Genes, Shanghai Cancer Institute, Renji Hospital, Shanghai Jiao Tong University School of Medicine, Shanghai, China

ARTICLE INFO

Keywords:
Hepatic steatosis
Ras activation
CPT1α
DNA damage
Hepatocarcinogenesis

ABSTRACT

Aberrant activation of the RAS cascade ubiquitously occurs in human hepatocellular carcinomas (HCC), regardless of rare mutations of RAS. However, the association between the Ras cascade and hepatic steatosis during hepatocarcinogenesis remains under-investigated. Here, the variation in the constitutive activity of Ras signaling and HCC incidence was found in a nonalcoholic fatty liver disease (NAFLD)-HCC mouse model, and Ras activity was induced by hepatic steatosis. Even in hepatocyte-specific expression of $Kras^{G12D}$ (Alb-Cre/$Kras^{G12D}$, $Kras^{hep}$) mice, mutagenic activation of Ras signaling was still significantly enhanced by NAFLD, with down-regulation of negative regulators. Interestingly, hepatic steatosis could be alleviated by persistent activation of Ras, whereas Ras accelerated DNA damage and HCC progression through Carnitine palmitoyltransferase 1A (CPT1α). A close correlation between active Ras and CPT1α was also shown in clinical steatosis peri-tumor tissues of HCC samples and experimental models. CPT1α inhibitor etomoxir (ETO) largely ameliorated active Ras-drived HCC. These findings can provide a novel link between steatosis and Ras activity in liver cancer.

1. Introduction

Hepatocellular carcinoma (HCC) is the sixth most common cancer and the second leading cause of cancer-related mortality worldwide, causing 745,000 deaths yearly [1]. Although the molecular pathogenesis of HCC is still unclear, the risk factors might be attributed to chronic viral infections, abnormal metabolisms and hepatotoxic agents. HCC occurrence is a complicated process which, like other solid tumors, involves cumulative genetic and epigenetic events, inactivation of tumor suppressor genes (eg, *Rb*, *p53*, *M6P/IGF2*, *E-cadherin*) and activation of oncogenic genes (eg, *c-Myc*, *Cyclin D1*, and *β-catenin*) [2–4]. Broad mutations have been revealed in HCC, but few are expected to be driver mutations [5,6].

Five major signaling cascades, including Wnt, TP53, Ras signaling, oxidative stress, and chromatin remodeling, have been reported to cover the most relevant molecular alterations in HCC [5]. Abnormal activation of the Ras pathways were identified in HCC [5–8], despite a rare occurrence of *B-Raf*, *H-Ras*, or *K-Ras* mutations [9,10], which are common in other tumors [11,12]. However, whether and/or how Ras activation defines oncogenic addiction loops in human HCC remains unclear.

Nonalcoholic fatty liver disease (NAFLD) is an independent risk factor for HCC, which is growing rapidly due to the prevalence of obesity and diabetes [4,13]. The occurrence of NAFLD and liver cancer is closely correlated with the abnormalities of hepatic lipid metabolism and dysregulation of relevant genes [14]. Akt/mTOR pathway is a major inducer of lipogenesis to promote HCC development [15]. However, despite the role of Ras as the upstream of Akt/mTOR, a systematic analysis of the Ras activation in NAFLD-HCC transition has not been reported.

In our studies, the HCC incidence was uneven although all the mice were treated with high-fat diets (HFDs) plus diethylnitrosamine (DEN) to induce NAFLD-HCC transition. The liver tissues with more HCCs displayed extensive Ras activity than those with fewer HCCs did.

* Corresponding author. 225 Changhai Road, Shanghai, 200438, China.
** Corresponding author. 225 Changhai Road, Shanghai, 200438, China.
E-mail addresses: chyyn2003@163.com (Y. Chen), hywangk@vip.sina.com (H. Wang).
[1] These authors contributed equally to this work.

https://doi.org/10.1016/j.canlet.2018.10.024
Received 1 August 2018; Received in revised form 6 October 2018; Accepted 17 October 2018

Abbreviations

8-OHdG	8-hydroxydeoxyguanosine
AFP	alpha fetal protein
AP	apurinic/apyrimidinic
ATGL	adipose triglyceride lipase
CPT1α	carnitine palmitoyl transferase 1A
CK19	cytokeratin 19
DEN	diethylnitrosamine
EpCAM	epithelial cell adhesion molecule
GCLM	glutamate-cysteine ligase modifier subunit
GTP	guanosine triphosphate
HCC	hepatocellular carcinoma
HFD	high-fat diet
MDA	malondialdehyde
NAFLD	nonalcoholic fatty liver disease
ND	normal diet
NQO1	NADPH quinone dehydrogenase 1
NRF2	nuclear factor erythroid 2-related factor 2
PCNA	proliferating cell nuclear antigen
p-ERK	phosphor-extracellular signal-regulated kinase
PPAR	peroxisome proliferator-activated receptors
ROS	reactive oxygen species

Consumption of HFD in wild type mice increased the levels of Ras activity, and that in mice with hepatic persistent activation of Ras (Alb-Kras^{G12D}, Kras^{hep}) developed abnormal hepatic lipid metabolism to promote hepatocarcinogenesis.

2. Materials and methods

2.1. Genetically engineered transgenic mice and treatments in animals

LSL-Kras^{G12D} mouse was a gift from Xiao Yang (Genetic Laboratory of Development and Diseases, Institute of Biotechnology, Beijing, China), and crossed with liver-specific Cre (albumin, Alb-Cre) mice to generate Alb-Kras^{G12D} mice (Kras^{hep}). It was kept in the barrier facility under pathogen-free conditions. All the animal experiments were conducted in accordance with the Guide for the Care and Use of Laboratory Animals. All the mice were maintained in filter topped cages on autoclaved regular chow diet (normal diet, ND, or high-fat diet, HFD, composed of 60%-fat, 14.1%-protein, and 25.9%-carbohydrates based on caloric content; TROPHIC). In the DEN-induced HCC model, DEN (25 mg/kg) was injected intraperitoneally into 15 days old mice [16,17]. After 8 weeks, mice were separated into two dietary groups and fed either ND or HFD for 17 weeks until they were sacrificed. In the Kras^{hep} HCC model, mice at 8 weeks of age were fed with ND or HFD for 16 or 20 weeks until they were sacrificed.

2.2. Clinical HCC specimens

Samples were collected from patients diagnosed with HCC who underwent curative resection without any adjuvant therapy before. Each of the 47 samples was pathologically diagnosed as HCC in the tumor region and steatosis in the peri-tumor region. The study has been approved by the Research Ethics Committee of Eastern Hepatobiliary Surgery Hospital, and the informed consent has been obtained.

2.3. Western blot

Liver tissues or primary hepatocytes were homogenized in RIPA (Sigma-Aldrich) lysis buffer with a protease (P001, NCM Biotech) and a phosphatase inhibitor cocktail (P003, NCM Biotech), separated on SDS-PAGE gels (P40650, NCM Biotech) and transferred onto Nitrocellulose membranes, which were blocked with 0.5% BSA and then immunoblotted with following antibodies: ACC1(1:2000; abcam; no.72046), ACC2 (1:2000; abcam; no.45174), Nrf2 (1:1000; Sigma; SAB2701989), GCLM (1:1000; Abclonal; A5314), NQO1 (1:1000; Abclonal; A0047), p-ACC (1:1,000, Beyotime, no. AA110), SREBP1 (1:500, abcam, no. 28481), P-SREBP1 (1:1000, CST, no. 9874), SCD1 (1:1000, abcam, no. 19862), CPT1α (1:1000, abcam, no. 128568), PPARγ (1:1000, CST, no. 2435), PPARα (1:1000; abcam; no. 8934), ATGL (1:1000; CST; no. 2439), ACOX (1:1000, abcam, no.184032), p-H_2AX (1:1000; CST; no. 9718), p53BP1(1:1000; abcam; no.175933), GCLM (1:1000, abclonal; no. A13989), cleaved-PARP (1:1000,abcam,no.32064), cleaved-Caspase3 (1:1000; abcam; no. 13847), CyclinD1 (1:1000; abclonal; no. A10757), PCNA (1:1000, abclonal, no.A9909), HSP90 (1:1000; abcam; no. 13492), β-actin (1:5000, abcam, no.8227); Anti-rabbit or anti-mouse horseradish peroxidase conjugated secondary antibody (1:4000; Zhongshan Biotech, ZB-2301 and ZB-2305) and ECL reagents (Engreen, 29050) were used to detect the signal.

Nucleus was isolated in line with the protocol of nuclear extraction kit (Thermos Scientific™).

2.4. Ras activity assay

Fresh liver samples from mice were preserved in DMEM medium (L110, Basalmedia) containing 10% fetal bovine serum (A100, H&X Biological Technology Co. Ltd), washed in D-Hanks (B430, Basalmedia). Ras activity was then assayed by Cell Biolabs' 96-well Ras Activation ELISA Kit (Cell Biolab Co. Ltd, STA-440). In brief, plate-bound Raf-1 RBD was utilized in this kit to selectively isolate and pull-down the active forms of Ras from purified samples or endogenous lysates. Subsequently, the captured GTP-Ras is detected by an Anti-pan-Ras Antibody and HRP conjugated secondary antibody.

2.5. Immunohistochemistry

Immunohistochemistry analysis was performed on 5 μm paraffin-embedded sections. Antigen retrieval of sections was performed in citrate buffer (pH 6.0) using a pressure cooker (Biocare Medical, DC2008). Then endogenous peroxidase activity was quenched by treatment with 3% H_2O_2 for 20 min. Sections were then blocked with normal serum for 60 min. The following antibodies were used: AFP (1:100, Proteintech, no.14550-1-AP); CK19 (1:500,Proteintech,10712-1-AP); Epcam (1:200, Abcam, no.71916); CD90 (1:500, CST, no.13801); CD105 (1:200, Abcam, no.107595); CD44 (1:100,BD Biosciences, San Jose, CA, USA); Ki67 (1:500, Abcam, no. 15580); 8OHDG (1:50, JalCA, no.MOG20); Malondialdehyde (1:1000, Abcam, no.6463); P53BP1 (1:100, Abcam, no.175933); S100A9 (1:100, Abcam, no.105472); CPT1α (1:2000, abcam, no. 128568); PPARγ (1:800, CST, no. 2435); CD68 (1:100, AbDSerotec no.MCA1957) and F4/80 (1:50, BIO RAD, no. MCA497R). The primary antibodies were incubated at 4 °C overnight. HRP-conjugated secondary antibodies (Zhong shan Biotech, DS-0001, PV-6001, PV-9001 or PV-9003) were then applied at 37 °C for 1 h, and immunoreactive cells were visualized with DAB (Immunohistochemistry, HRP, Zhongshan Biotech, ZLI-9019). Counterstaining was performed with hematoxylin (Sigma, St Louis, MO). Under high-power magnification (× 200), photographs of three representative fields were captured randomly and analyzed by the Image-Pro Plus v6.0 software (Media Cybernetics Inc, Bethesda, MD).

2.6. Metabolic measurements

Animals were monitored automatically for food consumption and

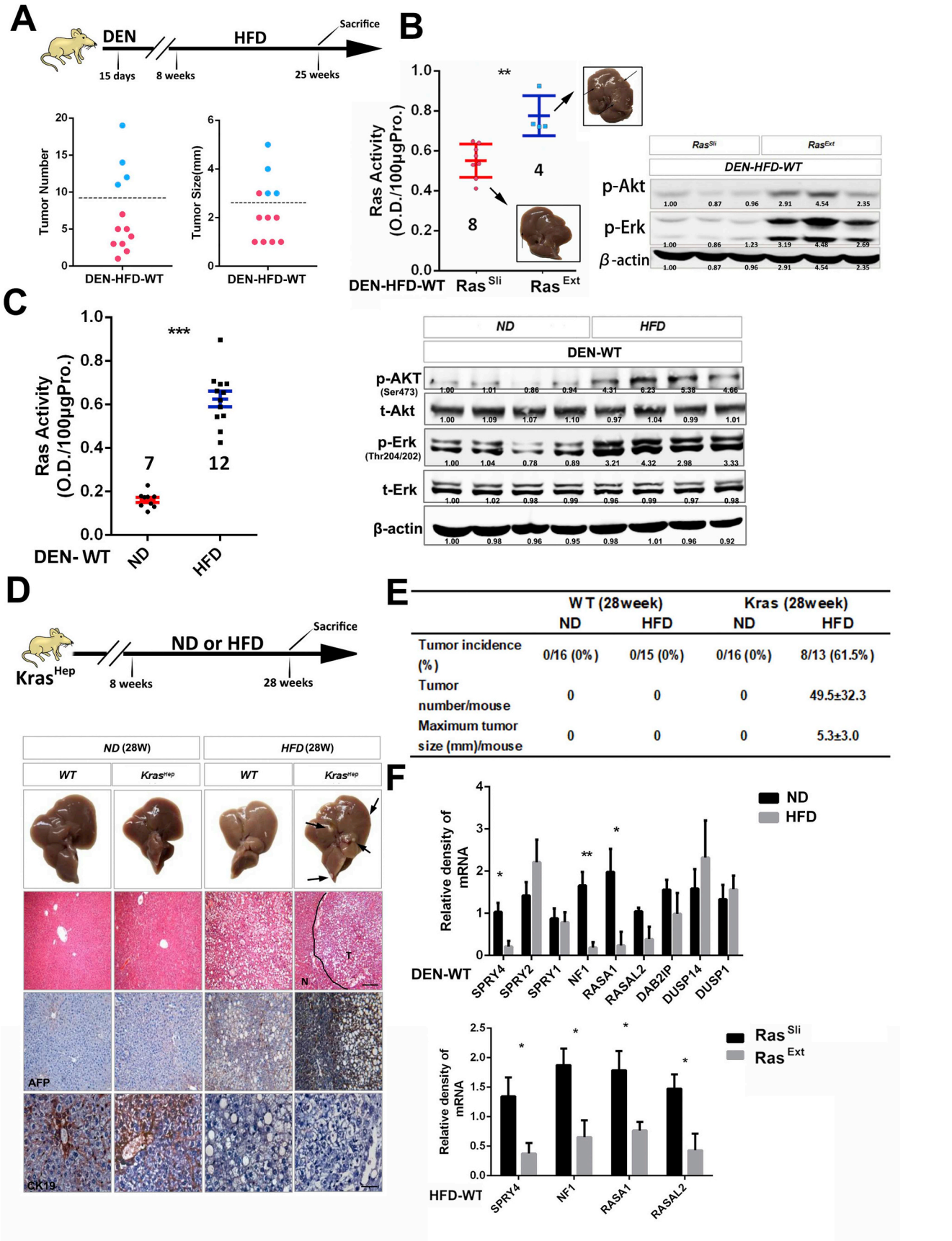

	WT (28week)		Kras (28week)	
	ND	HFD	ND	HFD
Tumor incidence (%)	0/16 (0%)	0/15 (0%)	0/16 (0%)	8/13 (61.5%)
Tumor number/mouse	0	0	0	49.5±32.3
Maximum tumor size (mm)/mouse	0	0	0	5.3±3.0

(caption on next page)

Fig. 1. NAFLD is an inducer of the Ras cascade and active Ras propels NAFLD-HCC transition.
A. Schematic representation of DEN-HFD-treated wild type mice. At 15 days of age, mice were injected with DEN and placed on HFD at 8 weeks of age for 17 weeks (top) (n = 12). Tumor burdens were detected and divided into two groups according to the tumor numbers, more HCCs (blue spots) and fewer HCCs (red spots).
B. Ras activity was compared between the blue and red groups (A), then divided into an extensive activation of Ras group (Ras^{ext}) and a slight activation of Ras one (Ras^{sli}). Gross anatomy of the representative livers in both two groups, with the latter showing macroscopic tumor nodules (black arrowhead). Immunoblot analysis of p-Akt, p-Erk and β-actin (A) (right).
C. Ras activity was assessed in DEN-ND or -HFD mouse model (left) (n = 7, ND group; n = 12, HFD group). Immunoblot analysis of p-Akt, t-Akt, p-Erk, t-Erk and β-actin in liver tissues (right).
D. Schematic representation of ND- or HFD-WT or -$Kras^{hep}$ mice for 20 weeks (top). Gross anatomy of the representative livers and macroscopic tumor nodules (black arrowhead) were shown in those mice.
E. Tumor incidences and burdens were compared among the above groups (D).
F. Expression analysis of negative regulators of Ras activity were measured in ND/HFD-wild type mice (top), or in HFD-Ras^{Ext} and -Ras^{Sli} groups (bottom) by real-time PCR.
Compared using Student's *t*-test, *p < 0.05, **p < 0.01, ***p < 0.001. (For interpretation of the references to colour in this figure legend, the reader is referred to the Web version of this article.)

metabolic measurements. For O_2 consumption and CO_2 production, mice were housed in metabolic cages placed inside a climate chamber. Gas concentrations were measured by sucking compressed air through custom-made metabolic chambers (flow rate of 0.45 L/min). The O_2 and CO_2 content of the individual animals were recorded by using O_2 and CO_2 analyzers (TSE-System, Bad Humburg, Germany). Oxygen consumption (VO_2) and carbon dioxide production (VCO_2) were calculated accordingly: VO_2 = Flow ML × (V1 + V2)/(N2Ref × Animal Weight × 100.0) and VCO_2 = Flow ML × dCO_2/(Animal Weight × 100.0); specific heat capacity at the constant volume of oxygen (CVO_2) and carbon dioxide production ($CVCO_2$) were calculated according to the temperature; respiratory exchange rate was calculated: RER = VCO_2/VO_2. Heat production (HP) was calculated accordingly: HP = ($CVO_2 \times VO_2 + CVCO_2 \times VCO_2$)/1000. Data were collected every 1 h over 12-h dark and 12-h light cycles.

2.7. ETO treatment

DEN (25 mg/kg) was injected intraperitoneally into 15 days old mice. After 8 weeks, mice were fed HFD until sacrificed. Five weeks after HFD was fed, mice were respectively randomized into two groups and treated with etomoxir (ETO) (S8244, Selleck) (40 mg/kg i.p. every other day for 5 weeks) or saline as untreated vehicle. The weight of these mice was recorded at the indicated time point.

2.8. Oil red O staining and DNA damage detection

Lipid accumulation was detected by Oil Red O staining in frozen liver sections with custom service of Histo Serv (Germantown, Maryland). Formation of apurinic or apyrimidinic (AP) sites in hepatocytes were tested with the kit (Dojindo Laboratories, DK02). In brief, the process included purification of genomic DNA, preparation of ARP-labeled DNA and determination of the number of basic sites in DNA.

2.9. ROS and antioxidants detection

Homogenate of fresh liver sections from WT or $Kras^{hep}$ mice was cultured with DCF (Thermo, D399) or Mito SOX (Thermo, M36008) for 30min, detected in the Microplate reader, and calibrated by protein concentration. GSSG, GSH and MDA were detected according to the protocol of the kits (Nanjing Jiancheng Bioengineering Institute, A061 and A003).

2.10. Statistical analysis

All the values presented are expressed as mean ± SD. χ^2 test and Student's t-test were applied to determine statistical significance. A value of P < 0.05 was considered significant (*P < 0.05, **P < 0.01, ***P < 0.001). Data analysis was performed by the SPSS software (version 16; SPSS).

3. Results

3.1. Ras signaling is constitutively activated during NAFLD-HCC transition, and also induced by hepatic steatosis

In DEN-HFD-induced NAFLD-HCC mouse model [16,17], the HCC incidence, unexpectedly, was not uniform for all wild type (WT) male mice, because 25% of the mice (4/12) showed more HCC lesions and larger sizes than others did (8/12, 75%) (Fig. 1A). Normally, Ras is inactive due to loading guanosine diphosphate (GDP), and transiently activated by intrinsic guanosine triphosphate (GTP) hydrolysis under stimuli. Intriguingly, those mice with more HCCs had obviously higher levels of constitutive activity of Ras signaling (Akt and Erk) than those with fewer HCCs did (Fig. 1B). These experimental groups were divided into an extensive activation of Ras group (Ras^{ext}) and a slight activation of Ras one (Ras^{sli}). It seemed an aberrant activation of Ras cascade in NAFLD-HCC transition.

We examined the constitutive activity of Ras signaling in the HFD-induced NAFLD mice model. Compared with normal diet (ND), DEN-HFD treatment (Fig.1C and Fig. S1B) or HFD along (Fig. S1C) led to a significant elevation of Ras signaling (Akt, mTOR, Erk and S6K) in liver tissues of WT mice. Together, it indicated that an abnormal activation of the Ras cascade also occurs in the presence of wild-type *Ras* genes in NAFLD.

3.2. Persistent Ras activation accelerated steatosis-mediated HCC progression

Regardless of the low rate at which mutations of *RAS* gene are activated in human HCC, uncontrolled activation of the *RAS* cascade may constitute a dominant oncogenic event [7,10,11]. Because of the essential role of *Kras* in mouse embryonic development and the limitation of directly targeting Ras activity [18–20], we used Alb-Cre/$Kras^{G12D}$ ($Kras^{hep}$) mice to cause persistent activation of Ras signaling, and study its role in NAFLD-HCC transition. On the other hand, *KRAS* mutations have been discovered in about 7% of human liver cancers, which are more common than *HRAS* and *NRAS* mutations [21]. Neither *Nras* nor *Hras* mutation in mice is powerful enough to induce HCC [22]. Specific expression of Kras in the liver (Fig. S1A) displayed some degrees of constitutively active Ras under ND feeding, but was remarkably elevated under HFD doing (Figs. S1B–F). After 25 weeks of DEN-ND/HFD treatment, both ND- and HFD-fed $Kras^{hep}$ mice grew tumors, but HFD-$Kras^{hep}$ mice exhibited far more HCCs per liver (42.4 ± 3.9 vs. 8 ± 2.6, $P < 0.0001$) than ND-$Kras^{hep}$ did (Figs. S2A,B, C), accompanied by an elevation of cancer stem cell markers including epithelial cell adhesion molecule (EpCAM), CD44, CD105 and CD90 (Figs. S2D and E). Moreover, even when all ND- and HFD-WT groups had no tumors at 18 weeks after DEN treatment, 85.7% (6/7) of the HFD-$Kras^{hep}$ mice exhibited massive nodules with a size ranging from 1 to 5 mm and the number ranging from 5 to 11 per mouse (Figs. S2B and C). Thus,

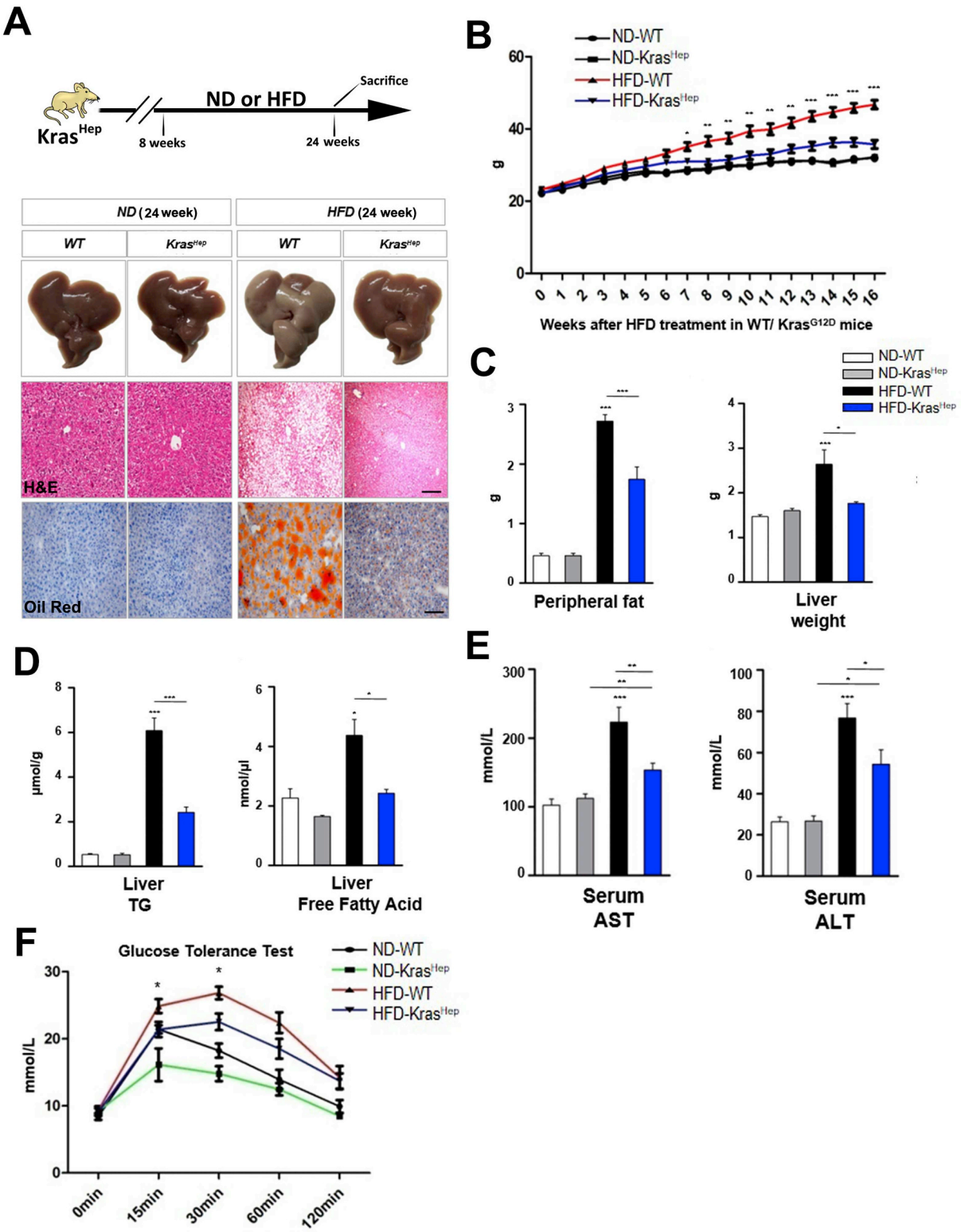

Fig. 2. Hepatic steatosis could be relieved by extensive Ras activation in HFD-Kras^{hep} mice.

A. Gross anatomy of the representative livers of 24-weeks ND- or HFD-Kras^{hep} mice prior to HCC formation were shown, as well as the representative H&E staining (Scale bars: 200 μm) or oil red O staining (Scale bars: 100 μm)

B. Weight curves of Kras^{hep} mice and WT littermates on a ND and a HFD (n = 8 mice/group).

C. Inguinal fat pad (left) or liver (right) weight were measured.

D. Liver triglyceride (TG) and liver free fatty acid were determined.

E. Serum aspartate transaminase (AST) and alanine transaminase (ALT) concentrations were determined.

F. Glucose tolerance test were performed (n = 4, ND-WT; n = 5, HFD-WT; n = 4, ND-Kras^{hep}; n = 5, HFD-Kras^{hep}).

Compared using Student's *t*-test, *p < 0.05, **p < 0.01, ***p < 0.001. (For interpretation of the references to colour in this figure legend, the reader is referred to the Web version of this article.)

persistent active Ras accelerated NAFLD-HCC transition.

Given the possibility of DEN as a genotoxic carcinogen directly or indirectly activating Ras or its downstream pathway, eight-week-old Kras^{hep} or control mice were treated with ND/HFD feeding alone for 20 weeks to determine the effect of steatosis-activated Ras on HCC occurrence. In contrast to ND-Kras^{hep} group without any tumors at 28 weeks, 61.5% (8/13) of HFD-Kras^{hep} mice exhibited massive nodules with the size ranging from 1 to 11 mm and the tumor number ranging from 10 to 87 per mouse (Fig. 1D and E). Persistent activation of oncogenic K-Ras in the liver, specific point mutation in codon 12, caused intrahepatic cholangiocarcinoma (ICC) and HCC [23,24]. In our study, immunohistochemical analysis of those tumor lesions revealed them as positive for alpha fetal protein (AFP) but negative for cytokeratin 19 (CK19), indicating the occurrence of HCC but not ICC in this model (Fig. 1D). Furthermore, 39.5% (17/43) of these tumors were fat vacuole-, solid- and fibrosis-like poorly differentiated tumors (Fig. S3A). Consistently, HFD-Kras^{hep} group had a higher liver body ratio, serum ALT and AST levels (Figs. S3B and C).

The RAS pathway was also hyperactivated in a subset of tumors that lacked the known oncogenic mutations [7,25]. Even in Kras^{hep} mice, which contained a constitutively active mutation of Ras, the basal state of Ras activity was not expectedly so higher than that in WT mice (Figs. S1B and C), but was clearly hyperactivated under HFD feeding (Figs. S1B and C). It seemed that some negative regulators of Ras activity might have been dismantled by NAFLD. Here, a panel of known negative regulators of the Ras pathway, such as sprout RTK signaling antagonist (SPRY)4, SPRY2, SPRY1, neurofibromin (NF)1, RAS p21 protein activator (RASA)1, RAS protein activator like (RASAL)2, DAB2 interacting protein (DAB2IP), dual specificity phosphatase (DUSP)14 and DUSP1, were further analyzed in WT mice under DEN-HFD or HFD alone conditions. Interestingly, DEN-HFD treatment led to transcriptional downregulations of *SPRY4*, *NF1*, and *RASA1* (Fig. 1F, upper panel). HFD alone treatment caused downregulations of the triple genes and *RASAL2* (Fig. 1F, down panel). Together, it suggested that HFD-induced NAFLD acts as an alternative inducer for Ras signaling to get involved in liver tumorigenesis.

3.3. Hepatic steatosis was alleviated by persistent Ras activation, but metabolic rate was enhanced

Obesity-caused chronic inflammation may increase the risk of HCC [16]. In our study, despite increased inflammation under DEN-HFD

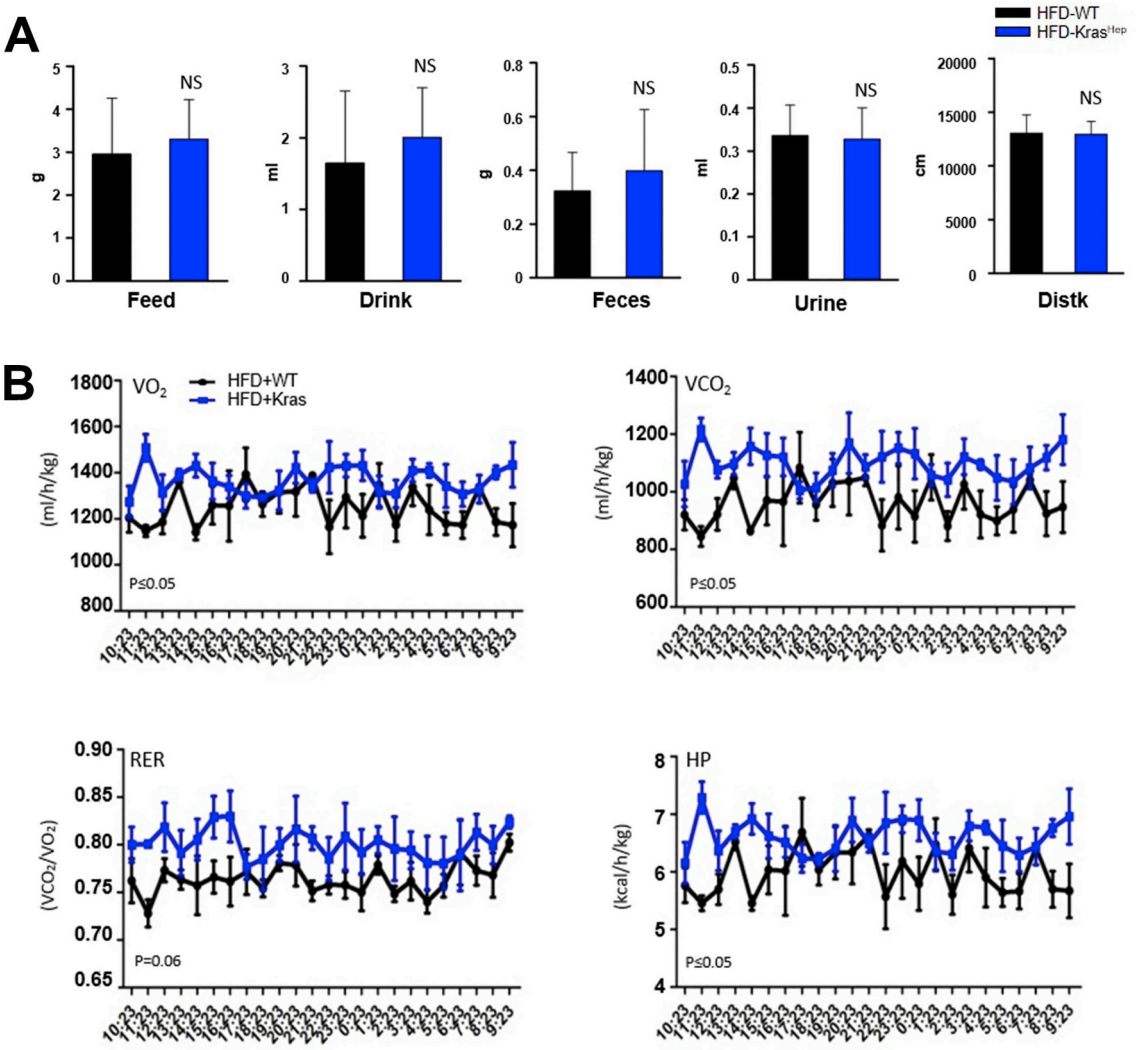

Fig. 3. HFD-Kras^{hep} mice displayed hypermetabolic rates.
A. HFD-WT and -Kras^{hep} were housed individually in cages over 3 days ad libitum and food consumption, drink consumption, feces production, urine production, and movement distance were recorded. (n = 3 mice/group).
B. Wild-type and Kras^{hep} on a HFD were housed in metabolic chambers. VO_2 consumption, VCO_2 production, respiratory exchange rate (RER), and heat production (HP) were measured over 24 h (12-h light and 12-h dark cycle). (n = 3 mice/group).

conditions, the two groups presented no statistical difference (Figs. S4A–C), implying that long-term HFD feeding-induced inflammation was coordinated with, but not dependent on, active Ras to contribute to HCC development. Liver fat accumulation or obesity-induced hepatosteatosis was associated with HCC development [16,26,27]. In the DEN-HFD-induced NAFLD-HCC transition model, WT mice showed excess hepatosteatosis and HCC occurrence at 25 weeks (Figs. S2B and C). However, despite increased HCC, nearly all the Kras^{hep} mice showed moderate liver fat at this time (Fig. S2B). Even before HCC formation in WT mice at 18 weeks of DEN-HFD, Kras^{hep} mice also presented HCC lesions but less liver fat (Fig. S2B). Next, because tumor cells likely utilize lipid for rapid growth, removal of DEN and sample collection before HCC formation was performed to evaluate the effect of Kras on liver fat. Even when no visible HCC lesion was observed at 24 weeks, HFD-Kras^{hep} mice still presented slighter symptoms with less peripheral fat, liver weight, liver triglyceride and free fatty acids than HFD-littermate controls with serious NAFLD (Fig. 2A–D). Moreover, HFD-Kras^{hep} mice remained leaner at around week 7 (Fig. 2B). Consistently, prior to HCC formation, HFD-Kras^{hep} mice showed lower levels of serum ALT, AST, and blood glucose than HFD-WT mice did (Fig. 2E and F). Unexpectedly, no visible difference of serum and liver cholesterol and serum triglyceride (TG) levels was detected in either group (Figs. S3A–C). Together, it implied that persistent activation of Ras had alleviated hepatic steatosis.

To define how active Ras alleviated hepatic steatosis in mice, we checked the energy metabolism in Kras^{hep} mice and littermate controls. Both groups with no difference in body weight when kept on HFD feeding at early 5 weeks were housed individually in metabolic chambers for 24 h (12 h light cycle followed by 12 h dark cycle), and their metabolic rates were elucidated by indirect calorimetry. Interestingly, there was no significant difference in the daily consumption of food or drinking water, defecation, urination or moving distance between the two groups (Fig. 3A). However, HFD-Kras^{hep} showed significantly increased O_2 consumption and CO_2 production, enhanced respiratory

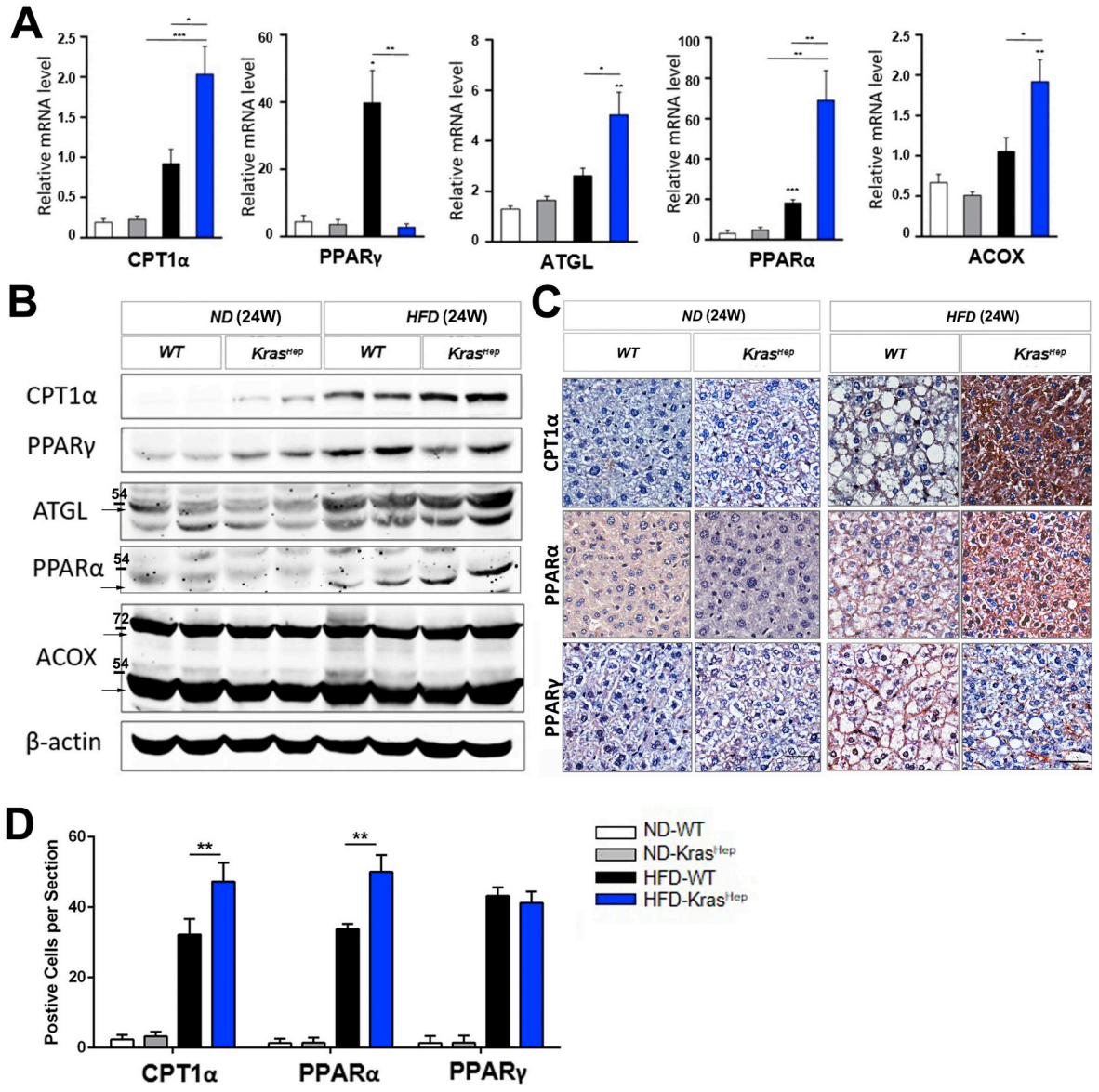

Fig. 4. The expressions of fatty acids β-oxidation-related genes were upregulated by active Ras in HFD-Kras^{hep} mice.
A&B. Expression analysis of genes involved in fatty acid β-oxidation (CPT1α, PPARγ, ATGL, PPARα and AOX) in the liver tissues of both HFD-wild type and -Kras^{hep} mice were measured by qRT-PCR (A) (n = 4) or western blot (B). β-actin was used as a loading control.
C&D. Immunohistochemistry analysis of CPT1α, PPARα and PPARγ staining in ND- or HFD-wild-type and -Kras^{hep}(C) and their quantifications (D). Scale bars: 50 μm. Compared using Student's *t*-test, *p < 0.05, **p < 0.01, ***p < 0.001.

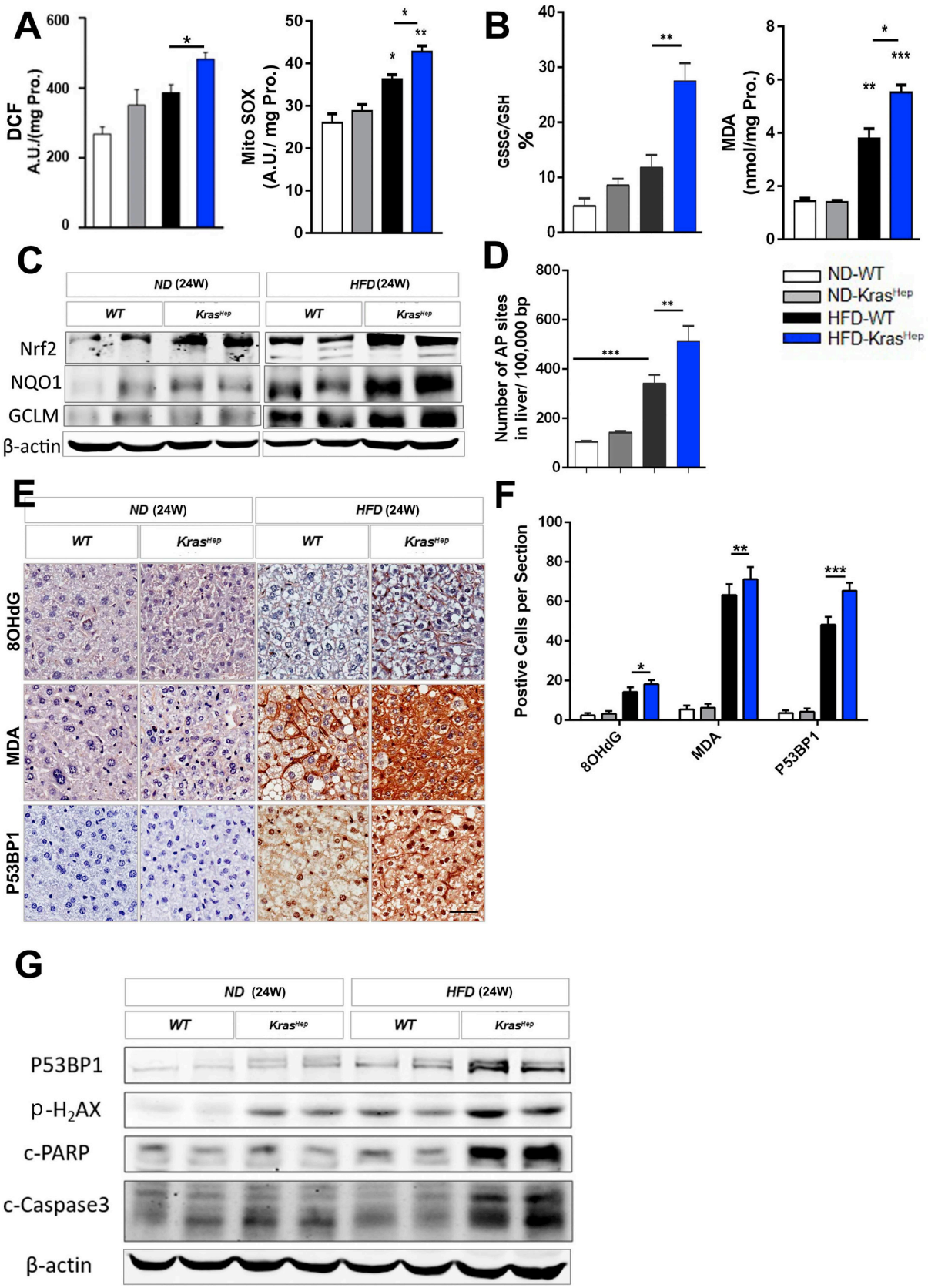

(caption on next page)

Fig. 5. Increased ROS and DNA damage in HFD-Kras^{hep} mice.
A. Quantification of cytoplasmic and mitochondrial ROS in liver sections of ND/HFD-WT and -Kras^{hep} mice was assessed by 2',7'-dichlorofluorescein (DCF) fluorescence or Mito SOX (n = 4). Meanwhile, their quantitative corrections were based on the total protein levels.
B. Quantification of oxidized GSH (Glutathione disulfide, GSSG for short)/total-GSH and malondialdehyde (MDA) (n = 4).
C. Immunoblot analysis of Nrf2, NQO1 and GCLM.
D. Detection of AP sites formation (n = 3).
E&F. Immunohistochemistry analysis of 8OHDG, MDA, P53BP1 in the tissues (E). Scale bars: 100 μm. Quantification of these molecule-positive cells are listed (F).
G. Immunoblot analysis of P53BP1, p-H_2AX, cleaved-PRAP and -caspase 3. β-actin was used as a loading control.
Compared using Student's *t*-test, *p < 0.05, **p < 0.01, ***p < 0.001.

exchange rate (RER: VCO_2/VO_2) and elevated thermogenesis (Fig. 3B), indicating that higher metabolic rates lessened lipid accumulation in HFD-Kras^{hep} mice.

3.4. Active Ras downregulated expression of lipogenic genes but upregulated expression of fatty acid β-oxidation genes

To further study the association of active Ras-improved steatosis with lipid metabolism, we examined the expression of lipid metabolism genes. The mRNA and protein levels of fatty acid synthesis genes, including acetyl-CoA carboxylase 1 (ACC1), acetyl-CoA carboxylase 2 (ACC2), fatty acid synthase (FASN), total and nuclear sterol regulatory element binding protein 1 (SREBP1), and stearoyl-Coenzyme A desaturase 1 (SCD1), were significantly downregulated in HFD-Kras^{hep} groups (Figs. S5A–B). In contrast, the transcriptions of fatty acid β-oxidation genes, carnitine palmitoyltransferase1α (CPT1α), adipose triglyceride lipase (ATGL), peroxisome proliferator-activated receptors α (PPARα) and monounsaturated fatty acid stearoyl-CoA (ACOX), were significantly elevated in HFD-Kras^{hep} groups, except for peroxisome proliferator-activated receptor γ (PPARγ) (Fig. 4A). Remarkably, immunoblot and immunostaining analysis showed the increased protein levels of PPARα and CPT1α (Fig. 4B–D). Collectively, it suggested that active Ras inhibited fatty acids synthesis (FAS) but promoted fatty acids oxidation (FAO), which led to a higher metabolic rate but lower lipid accumulation.

3.5. Active Ras intensified oxidative stresses and DNA damage

Persistent fatty acids oxidation results in hepatic mitochondrial dysfunction and peroxisomal fatty acid oxidation, which impairs lipid homeostasis, induces reactive oxygen species (ROS) and DNA damage [28–31]. Activated inflammatory cells release free radicals, such as ROS and nitric oxide reactive species (NOS), causing DNA damage and gene mutations, and thus fostering neoplastic transformation [32]. In this study, elevated ROS production accompanied by an increase of the GSSG/GSH ratio and methane dicarboxylic aldehyde (MDA) content was detected in HFD-Kras^{hep} mice (Fig. 5A and B). On the other hand, antioxidant associated proteins, including Nrf2, glutamate-cysteine ligase modifier subunit (GCLM), and NADPH quinone dehydrogenase 1 (NQO1), were also enhanced in HFD-Kras^{hep} mice (Fig. 5C), indicative of consequently strengthened antioxidant capacity. Moreover, assessment of apurinic/apyrimidinic (AP) sites formation and immunostaining of 8-Hydroxyguanosine (8OHdG) or MDA confirmed that active Ras enhanced HFD-mediated oxidative stress and DNA damage (Fig. 5D–F). However, the indicators of DNA damage response (p-H_2AX and P53BP1) and cleaved-PRAP and -caspase-3 were also increased in the HFD-Kras^{hep} group (Fig. 5E–G), which could be partially accounted for by the involvement of ROS in necrosis and apoptosis [33]. Taken together, these results strongly suggested that active Ras promoted hepatic lipid peroxidation and DNA damage, which coordinately contributed to neoplastic transformation.

3.6. Extensive Ras activation was associated with elevation of CPT1α and DNA damage in steatosis peri-tumor tissues of HCC specimens

We next collected 47 clinical HCC samples, which were pathologically diagnosed as HCC in the tumor region and steatosis in the peri-tumor region. These steatosis peri-tumor tissues were analyzed for the correlation of Ras activity with CPT1α and DNA damage levels. As with the results from DEN-HFD-induced HCC mouse model, these specimens were divided into two groups according to levels of Ras activity, one with Ras extensive activity (HCC-Ras^{Ext}) and the other with slight activity (HCC-Ras^{Sli}) (Fig. 6A). Accordingly, a significant elevation of CPT1α was detected in HCC-Ras^{Ext}, compared to ATGL and PPARγ (Fig. 6B and C). Partial increases of p-H_2AX and P53BP1 were also displayed in HCC-Ras^{Ext} (Fig. 6D). Similarly, in the DEN-HFD-induced HCC mouse model, CPT1α, PPARγ and p-H_2AX were upregulated, and DCF, GSH/GSSG, and AP site increased in HCC-Ras^{Ext} group (Fig. 6E–G). Together, it implied the pivotal effect of Ras activation on FAO and DNA damage in HCC.

3.7. CPT1α activity was required for the pathological effects of active Ras on HCC

Given the significant elevation of CPT1α in HFD-Kras^{hep} group, the inhibitor of CPT1α etomoxir (ETO) was then administrated *in vivo* to explore the involvement of CPT1α in this process. After 5 weeks of ETO treatment, all DEN-HFD-Kras^{hep} mice showed no obvious difference in body weight loss (Fig. 7A) or hepatic lipid accumulation (Figs. S6A–E), which partially excluded the toxicity of the drug in the short term. Notably, ETO administration markedly reduced the tumor numbers, the maximum diameters, and the serum levels of aminotransferases in DEN-HFD-Kras^{hep} mice (Fig. 7B–D). ETO treatment also diminished ROS production (Fig. 7E) and markedly lowered expressions of cell-cycle regulators (cyclin D1, PCNA), apoptosis markers (cleaved-caspase-3, cleaved-PARP), and DNA damage responsor p-H_2AX in DEN-HFD-Kras^{hep} mice (Fig. 7F). Together, these data suggested CPT1α involvement in the pathological effects of active Ras during hepatocarcinogenesis.

4. Discussion

NAFLD is one of the significant risk factors for HCC. In this study, long-term consumption of HFD-induced NAFLD caused Ras activation in the liver of WT mice, as evaluated by increased levels of Ras activity, p-Akt, and p-Erk. Moreover, extensive Ras activation was correlated with hepatocarcinogenesis in the NAFLD-HCC mouse model. Even in the Kras^{hep} mouse model with active hepatic Ras, HFD-induced steatosis could still further lead to induction of Ras signaling, and persistent Ras activation accelerated hepatocarcinogenesis. One limitation of the study was that the Kras models could only allow us to study the impact of oncogenic Ras on hepatic steatosis-HCC formation, rather than the blocking of Ras activity. Despite the possibility that farnesyl transferase inhibitors inhibit Ras, clinical trials have failed so far [34,35]. Their antitumor activity remains to be further studied [36]. Nevertheless, our experimental studies and clinical biopsies analysis strongly indicated active Ras as a crucial factor involved in the process.

Lipid metabolic reprograming is a key process during tumorigenesis, involving dysregulation of lipid metabolic process genes [14]. In current study, besides partial down-regulation of fatty acid synthesis genes, up-regulation of PPARα and CPT1α was presented in HFD-Kras^{hep} mice (Fig. S5, Fig. 4A–D). The latter plays a crucial role in fatty liver and its involvement in carcinogenesis has been clarified [37–39]. CPT1 has

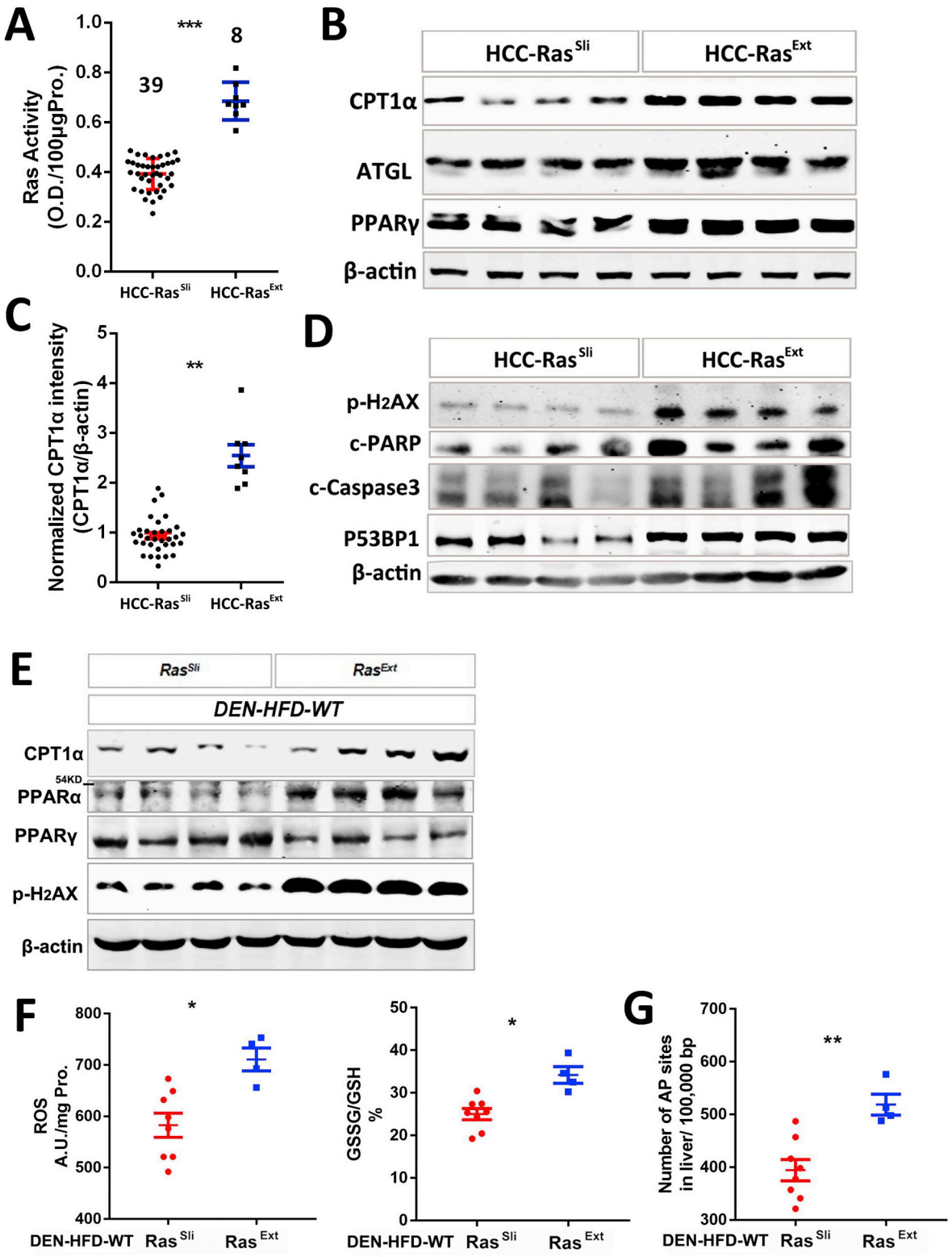

Fig. 6. Extensive activation of Ras associated with CPT1α and DNA damage in steatosis peri-tumor tissues of HCC specimens.

A. Steatosis peri-tumor tissues from forty-seven HCC patients were detected for Ras activities, and divided into two groups, one with Ras extensive activation (HCC-Ras^{Ext}) containing 9 patients, the other with Ras slight activation (HCC-Ras^{Sli}) containing 38 patients.

B&C. Immunoblot analysis of CPT1α, ATGL, PPARγ were shown (B), and the intensity of CPT1α were normalized by β-actin and compared in different groups (C).

D. Immunoblot analysis of P53BP1, p-H_2AX, cleaved-PRAP, or -caspase3.

E. Immunoblot analysis of CPT1α, PPARα, PPARγ and p-H_2AX in HFD-Ras^{Ext} and -Ras^{Sli} WT mice.

F. Quantification of cytoplasmic ROS by DCF and GSSH/GSH (E). Meanwhile, their quantitative correction was based on total proteins levels.

G. Detection of AP sites formation (E).

Compared using Student's *t*-test, *p < 0.05, **p < 0.01, ***p < 0.001.

been regarded as a therapeutic target for prostate, breast and ovarian cancers [37]. CPT1C, one isoform of CPT1, functions as a potential oncogene to prevent cell death from glucose limitation or hypoxia in lung cancer cells [39]. Our previous study proved CPT1α essential for HCC cell survival [38]. The clinical or experimental relevance of Ras activity to CPT1α expression is currently shown (Fig. 6B, C, E). Moreover, suppression of CPT1α blocked active Ras-promoted HCC formation. Lipid oxidation is required for some types of tumors as the main source of energy. High uptake of fatty acids or overexpression of some β-oxidation enzymes is generally displayed in prostate tumors [40,41].

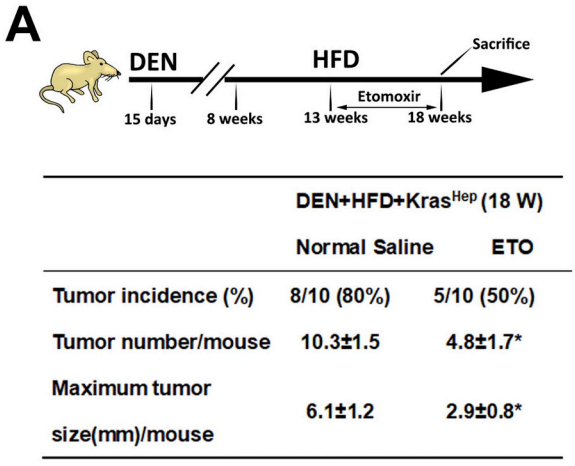

	DEN+HFD+Kras^{Hep} (18 W)	
	Normal Saline	ETO
Tumor incidence (%)	8/10 (80%)	5/10 (50%)
Tumor number/mouse	10.3±1.5	4.8±1.7*
Maximum tumor size(mm)/mouse	6.1±1.2	2.9±0.8*

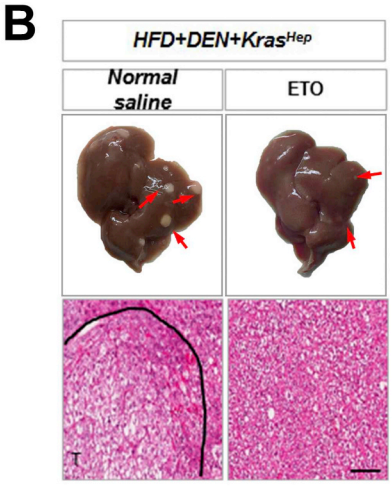

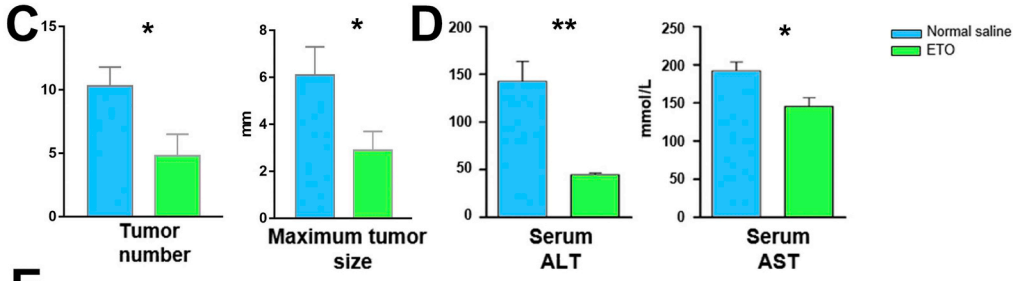

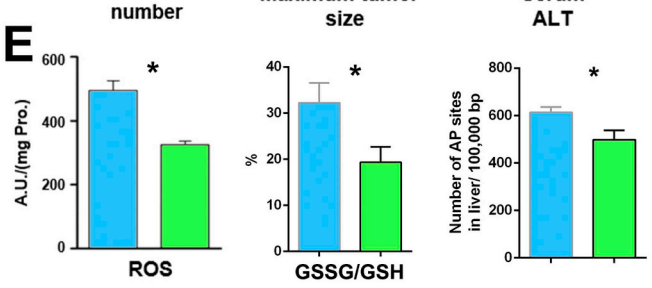

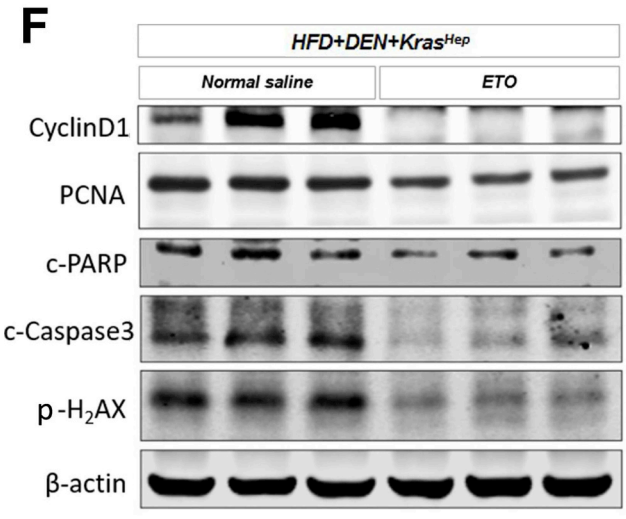

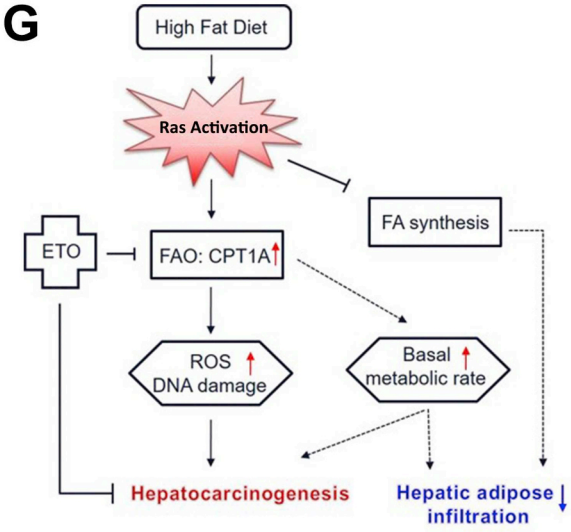

(caption on next page)

Fig. 7. Targeting CPT1α retarded HFD-Kras^{hep}-drove HCC formation.
A. Kras^{hep} mice were injected with a single DEN (25 mg/kg) at 15-days old, fed with HFD for 5 weeks at 8-weeks old, then randomly divided into the two groups: fed with HFD and simultaneously injected with saline or ETO (40 mg/kg), twice per week for 5 weeks. Body weight of each mouse was measured weekly (n = 10 mice/group).
B. Representative image of DEN-HFD-Kras^{hep} mice livers after normal saline or ETO injection. The macroscopic tumor nodules were shown by the arrowhead and H&E staining. Compared to ETO treatment, tumor (T) lesion clearly compressed the adjacent normal (N) liver tissue in HCC after normal saline treatment. Scale bars: 100 μm.
C–F. Tumor number and maximum tumor size (C), serum ALT and AST concentrations (D), quantification of ROS, GSSH/GSH and AP sites (E), and immunoblot analysis of CyclinD1, PCNA, γ-H2AX, cleaved-PRAP and -caspase3 (F) in normal saline or ETO-treated groups were determined at 10 weeks after HFD treatment (n = 10 mice/group). Meanwhile, their quantitative correction was based on total proteins levels. β-actin was used as a loading control.
G. Schematic depicting the role of active Ras in regulating fatty acid metabolism.
Compared using Student's *t*-test, *p < 0.05, **p < 0.01.

Therefore, a better understanding of these metabolic adaptations may warrant further exploitation for potential therapeutic benefits [42].

Little is known about the precise mechanism by which active Ras regulates CPT1α. P38 MAPK has been reported as a negative regulator of liver steatosis via upregulating PPARα and CPT1α [43]. Given p38 MAPK elevation in HFD-Kras^{hep} mice (Fig. S5C), we speculated p38 MAPK partial involvement in this regulation. In our study, activation of Akt/mTOR pathway but downregulation of fatty acid synthesis-related genes were shown in HFD-Kras^{hep} liver tissues, inconsistent with Calvisi et al. study that the Akt-mTOR-S6K promoted lipogenesis via transcriptional mechanism in human HCC [15]. Thus, in the HFD-Kras^{hep} mouse model, the regulation of lipogenic genes was likely to be independent of AKT/mTOR pathway. Additionally, less nuclear and total SREBP1 seemed paradoxical to activation of AKT/mTOR pathway in HFD-Kras^{hep} mice, indicating that some unknown factors might regulate SREBP1 rather than Akt/mTOR pathway.

A second limitation was lacking in-depth analysis in this study. Loss of negative regulators amplifies Ras signaling independently of genetic alterations in Ras genes, which play a causal role in human cancer [25,44,45]. Intriguingly, the variation in Ras activity and tumor growth was observed in wild type mice under HFD-DEN treatment. Even in DEN-HFD-Kras^{hep} mice, the basal state of Ras activity can still be externally induced by HFD feeding. One potential explanation is that the genome integrity was abolished by genotoxic DEN, which caused mutagenic action and variation of Ras inhibitors, but this divergence was further amplified by NAFLD. Some negative regulators of the Ras pathway were downregulated by NAFLD (Fig. 1F), suggesting that NAFLD, as an external stimulus, directly or indirectly activated Ras and inflammation before cooperatively promoting HCC. Despite the rare rate of activating mutations of RAS gene in human HCC [9], RAS cascade activation, including aberrant methylation of RAS inhibitors, occurs in HCC patients [10]. In our study, RAS extensive activation was displayed in eight of the forty-seven patients (17%) with HCC, indicating the possibility of upstream inducers, inactivation of RAS inhibitors, or other unknown factors leading to dysregulating RAS activity in HCC. Coincidentally, Calvisi et al. reported that inactivation of RAS inhibitory GAPs and PITX1 could cause RAS activation in HCC [7]. As for the complexity of epigenetic suppression of negative regulators and epigenetic amplification of RAS gene transcriptional output, the exact mechanism of steatosis-induced Ras activation needs to be clarified in the future. Regardless of a complex mixture of pathogenic factors and genetic background, RAS activation deserves attention in HCC. Sorafenib, the multikinase inhibitor drug approved for advanced HCC, targets both RAF/MEK/ERK pathway and VEGFR/PDGFR [46]. Rafametinib, the MEK inhibitor, also displays potential efficacy in treating HCC with RAS mutation [47]. Therefore, it becomes essential to reconsider targeting for RAS activity in HCC.

Of particular note, universal immunization against HBV and antiviral therapy for primary HCC prevention has consistently been associated with decreased HCC risk. Much attention has been paid to metabolic disorders, including obesity, NAFLD, and diabetes as the risk factors for HCC [48]. In our study, NAFLD-activated Ras and active Ras-accelerated NAFLD-HCC progression revealed the significance of active Ras in HCC even with few mutations. Taken together, our study highlighted a feed-forward loop for hepatocarcinogenesis: aberrant induction of Ras causes abnormal lipid metabolism. Targeting lipid metabolism may also offer novel therapeutic strategies for cancer treatment.

Grant support

Research was supported by the projects from National Natural Science Foundation of China (81522035, 81670568, 81521091, 81872231, 81472768, 91529306), the State Key Project for Infectious Diseases (2015ZX09J15107, 2017ZZ01007, AWS16J029), Shanghai Committee of Science and Technology (15431901600, 16QA1404900, 14XD1400100).

Author contributions

An Xu: acquisition of data, analysis and interpretation of data, and statistical analysis; Bibo Wang: analysis and interpretation of data and drafting of the manuscript; Jing Fu: acquisition of data; Ting Yu, Wenhao Qin, Zhishi Yang, Qingjun Lu and Jingyi Chen: manuscript editing; Yao Chen: study concept and design, analysis and interpretation of data, critical revision of the manuscript for important intellectual content, obtained study funding, and study supervision; Hongyang Wang: study concept and design, analysis and interpretation of data, drafting of the manuscript, critical revision of the manuscript for important intellectual content, obtained study funding, and study supervision. All authors have read and approved the manuscript for publication.

Conflicts of interest

The authors declare that they have no competing interests.

Acknowledgments

We thank Dong-Ping Hu, Lin-Na Guo, Dan Cao, Shan-Hua Tang, Dan-Dan Huang, Shan-Na Huang and Jing Peng for technical assistances. We also thank for Xiao Yang, Yan Teng and Xiu-Bin Li helpful suggestions.

Appendix A. Supplementary data

Supplementary data to this article can be found online at https://doi.org/10.1016/j.canlet.2018.10.024.

References

[1] L.A. Torre, F. Bray, R.L. Siegel, J. Ferlay, J. Lortet-Tieulent, A. Jemal, Global cancer statistics, 2012, CA A Cancer J. Clin. 65 (2015) 87–108.
[2] S.S. Thorgeirsson, J.W. Grisham, Molecular pathogenesis of human hepatocellular carcinoma, Nat. Genet. 31 (2002) 339–346.
[3] F. Feo, R.M. Pascale, M.M. Simile, M.R. De Miglio, M.R. Muroni, D. Calvisi, Genetic alterations in liver carcinogenesis: implications for new preventive and therapeutic strategies, Crit. Rev. Oncog. 11 (2000) 19–62.

[4] H.Y. Wang, Non-resolving inflammation and cancer, Sci. China Life Sci. 60 (2017) 561–562.
[5] C. Guichard, G. Amaddeo, S. Imbeaud, Y. Ladeiro, L. Pelletier, I.B. Maad, J. Calderaro, et al., Integrated analysis of somatic mutations and focal copy-number changes identifies key genes and pathways in hepatocellular carcinoma, Nat. Genet. 44 (2012) 694–698.
[6] Z. Kan, H. Zheng, X. Liu, S. Li, T.D. Barber, Z. Gong, H. Gao, et al., Whole-genome sequencing identifies recurrent mutations in hepatocellular carcinoma, Genome Res. 23 (2013) 1422–1433.
[7] D.F. Calvisi, S. Ladu, E.A. Conner, D. Seo, J.T. Hsieh, V.M. Factor, S.S. Thorgeirsson, Inactivation of Ras GTPase-activating proteins promotes unrestrained activity of wild-type Ras in human liver cancer, J. Hepatol. 54 (2011) 311–319.
[8] L.M. Guachalla, K.L. Rudolph, The GAPs between hepatocellular carcinoma and RAS, J. Hepatol. 54 (2011) 191–192.
[9] W. Hou, J. Liu, P. Chen, H. Wang, B.C. Ye, F. Qiang, Mutation analysis of key genes in RAS/RAF and PI3K/PTEN pathways in Chinese patients with hepatocellular carcinoma, Oncol. Lett. 8 (2014) 1249–1254.
[10] J.W. Grisham, Interspecies comparison of liver carcinogenesis: implications for cancer risk assessment, Carcinogenesis 18 (1997) 59–81.
[11] D.F. Calvisi, S. Ladu, A. Gorden, M. Farina, E.A. Conner, J.S. Lee, V.M. Factor, et al., Ubiquitous activation of Ras and Jak/Stat pathways in human HCC, Gastroenterology 130 (2006) 1117–1128.
[12] P. Newell, S. Toffanin, A. Villanueva, D.Y. Chiang, B. Minguez, L. Cabellos, R. Savic, et al., Ras pathway activation in hepatocellular carcinoma and anti-tumoral effect of combined sorafenib and rapamycin in vivo, J. Hepatol. 51 (2009) 725–733.
[13] C.D. Williams, J. Stengel, M.I. Asike, D.M. Torres, J. Shaw, M. Contreras, C.L. Landt, et al., Prevalence of nonalcoholic fatty liver disease and nonalcoholic steatohepatitis among a largely middle-aged population utilizing ultrasound and liver biopsy: a prospective study, Gastroenterology 140 (2011) 124–131.
[14] E. Currie, A. Schulze, R. Zechner, T.C. Walther, R.V. Farese Jr., Cellular fatty acid metabolism and cancer, Cell Metabol. 18 (2013) 153–161.
[15] D.F. Calvisi, C. Wang, C. Ho, S. Ladu, S.A. Lee, S. Mattu, G. Destefanis, et al., Increased lipogenesis, induced by AKT-mTORC1-RPS6 signaling, promotes development of human hepatocellular carcinoma, Gastroenterology 140 (2011) 1071–1083.
[16] E.J. Park, J.H. Lee, G.Y. Yu, G. He, S.R. Ali, R.G. Holzer, C.H. Osterreicher, et al., Dietary and genetic obesity promote liver inflammation and tumorigenesis by enhancing IL-6 and TNF expression, Cell 140 (2010) 197–208.
[17] X. Jin, D. Moskophidis, N.F. Mivechi, Heat shock transcription factor 1 is a key determinant of HCC development by regulating hepatic steatosis and metabolic syndrome, Cell Metabol. 14 (2011) 91–103.
[18] L. Johnson, D. Greenbaum, K. Cichowski, K. Mercer, E. Murphy, E. Schmitt, R.T. Bronson, et al., K-ras is an essential gene in the mouse with partial functional overlap with N-ras, Genes Dev. 11 (1997) 2468–2481.
[19] K. Koera, K. Nakamura, K. Nakao, J. Miyoshi, K. Toyoshima, T. Hatta, H. Otani, et al., K-ras is essential for the development of the mouse embryo, Oncogene 15 (1997) 1151–1159.
[20] S.J. Plowman, D.J. Williamson, M.J. O'Sullivan, J. Doig, A.M. Ritchie, D.J. Harrison, D.W. Melton, et al., While K-ras is essential for mouse development, expression of the K-ras 4A splice variant is dispensable, Mol. Cell Biol. 23 (2003) 9245–9250.
[21] S. Whittaker, R. Marais, A.X. Zhu, The role of signaling pathways in the development and treatment of hepatocellular carcinoma, Oncogene 29 (2010) 4989–5005.
[22] A.T. Baines, D. Xu, C.J. Der, Inhibition of Ras for cancer treatment: the search continues, Future Med. Chem. 3 (2011) 1787–1808.
[23] M.R. O'Dell, J.L. Huang, C.L. Whitney-Miller, V. Deshpande, P. Rothberg, V. Grose, R.M. Rossi, et al., Kras(G12D) and p53 mutation cause primary intrahepatic cholangiocarcinoma, Cancer Res. 72 (2012) 1557–1567.
[24] H. Ye, C. Zhang, B.J. Wang, X.H. Tan, W.P. Zhang, Y. Teng, X. Yang, Synergistic function of Kras mutation and HBx in initiation and progression of hepatocellular carcinoma in mice, Oncogene 33 (2014) 5133–5138.
[25] R. Lock, K. Cichowski, Loss of negative regulators amplifies RAS signaling, Nat. Genet. 47 (2015) 426–427.
[26] S.H. Caldwell, D.M. Crespo, H.S. Kang, A.M. Al-Osaimi, Obesity and hepatocellular carcinoma, Gastroenterology 127 (2004) S97–S103.
[27] H.B. El-Serag, K.L. Rudolph, Hepatocellular carcinoma: epidemiology and molecular carcinogenesis, Gastroenterology 132 (2007) 2557–2576.
[28] J. Zeng, S. Deng, Y. Wang, P. Li, L. Tang, Y. Pang, Specific inhibition of Acyl-CoA oxidase-1 by an acetylenic acid improves hepatic lipid and reactive oxygen species (ROS) metabolism in rats fed a high fat diet, J. Biol. Chem. 292 (2017) 3800–3809.
[29] H. Ishikawa, A. Takaki, R. Tsuzaki, T. Yasunaka, K. Koike, Y. Shimomura, H. Seki, et al., L-carnitine prevents progression of non-alcoholic steatohepatitis in a mouse model with upregulation of mitochondrial pathway, PloS One 9 (2014) e100627.
[30] H. Cortez-Pinto, J. Chatham, V.P. Chacko, C. Arnold, A. Rashid, A.M. Diehl, Alterations in liver ATP homeostasis in human nonalcoholic steatohepatitis: a pilot study, J. Am. Med. Assoc. 282 (1999) 1659–1664.
[31] G. Serviddio, F. Bellanti, R. Tamborra, T. Rollo, A.D. Romano, A.M. Giudetti, N. Capitanio, et al., Alterations of hepatic ATP homeostasis and respiratory chain during development of non-alcoholic steatohepatitis in a rodent model, Eur. J. Clin. Invest. 38 (2008) 245–252.
[32] S.F. Yang, C.W. Chang, R.J. Wei, Y.L. Shiue, S.N. Wang, Y.T. Yeh, Involvement of DNA damage response pathways in hepatocellular carcinoma, BioMed Res. Int. 2014 (2014) 153867.
[33] J. Wu, M.A. Zern, Hepatic stellate cells: a target for the treatment of liver fibrosis, J. Gastroenterol. 35 (2000) 665–672.
[34] A.E. Karnoub, R.A. Weinberg, Ras oncogenes: split personalities, Nat. Rev. Mol. Cell Biol. 9 (2008) 517–531.
[35] G.L. James, J.L. Goldstein, M.S. Brown, Polylysine and CVIM sequences of K-RasB dictate specificity of prenylation and confer resistance to benzodiazepine peptidomimetic in vitro, J. Biol. Chem. 270 (1995) 6221–6226.
[36] B. Rotblat, M. Ehrlich, R. Haklai, Y. Kloog, The Ras inhibitor farnesylthiosalicylic acid (Salirasib) disrupts the spatiotemporal localization of active Ras: a potential treatment for cancer, Methods Enzymol. 439 (2008) 467–489.
[37] H. Shao, E.M. Mohamed, G.G. Xu, M. Waters, K. Jing, Y. Ma, Y. Zhang, et al., Carnitine palmitoyltransferase 1A functions to repress FoxO transcription factors to allow cell cycle progression in ovarian cancer, Oncotarget 7 (2016) 3832–3846.
[38] M.D. Wang, H. Wu, G.B. Fu, H.L. Zhang, X. Zhou, L. Tang, L.W. Dong, et al., Acetyl-coenzyme A carboxylase alpha promotion of glucose-mediated fatty acid synthesis enhances survival of hepatocellular carcinoma in mice and patients, Hepatology 63 (2016) 1272–1286.
[39] H.S. Zimbler-Delorenzo, F.S. Dobson, Demography of squirrel monkeys (Saimiri sciureus) in captive environments and its effect on population growth, Am. J. Primatol. 73 (2011) 1041–1050.
[40] P.J. Effert, R. Bares, S. Handt, J.M. Wolff, U. Bull, G. Jakse, Metabolic imaging of untreated prostate cancer by positron emission tomography with 18fluorine-labeled deoxyglucose, J. Urol. 155 (1996) 994–998.
[41] S. Zha, S. Ferdinandusse, J.L. Hicks, S. Denis, T.A. Dunn, R.J. Wanders, J. Luo, et al., Peroxisomal branched chain fatty acid beta-oxidation pathway is upregulated in prostate cancer, Prostate 63 (2005) 316–323.
[42] P.P. Hsu, D.M. Sabatini, Cancer cell metabolism: warburg and beyond, Cell 134 (2008) 703–707.
[43] Y. Xiao, J. Wang, W. Yan, K. Zhou, Y. Cao, W. Cai, p38alpha MAPK antagonizing JNK to control the hepatic fat accumulation in pediatric patients onset intestinal failure, Cell Death Dis. 8 (2017) e3110.
[44] G. Hrustanovic, V. Olivas, E. Pazarentzos, A. Tulpule, S. Asthana, C.M. Blakely, R.A. Okimoto, et al., RAS-MAPK dependence underlies a rational polytherapy strategy in EML4-ALK-positive lung cancer, Nat. Med. 21 (2015) 1038–1047.
[45] R.W. Wiseman, S.J. Stowers, E.C. Miller, M.W. Anderson, J.A. Miller, Activating mutations of the c-Ha-ras protooncogene in chemically induced hepatomas of the male B6C3 F1 mouse, Proc. Natl. Acad. Sci. U. S. A. 83 (1986) 5825–5829.
[46] L. Liu, Y. Cao, C. Chen, X. Zhang, A. McNabola, D. Wilkie, S. Wilhelm, et al., Sorafenib blocks the RAF/MEK/ERK pathway, inhibits tumor angiogenesis, and induces tumor cell apoptosis in hepatocellular carcinoma model PLC/PRF/5, Cancer Res. 66 (2006) 11851–11858.
[47] H.Y. Lim, J. Heo, H.J. Choi, C.Y. Lin, J.H. Yoon, C. Hsu, K.M. Rau, et al., A phase II study of the efficacy and safety of the combination therapy of the MEK inhibitor refametinib (BAY 86-9766) plus sorafenib for Asian patients with unresectable hepatocellular carcinoma, Clin. Canc. Res. 20 (2014) 5976–5985.
[48] Z.M. Younossi, M. Otgonsuren, L. Henry, C. Venkatesan, A. Mishra, M. Erario, S. Hunt, Association of nonalcoholic fatty liver disease (NAFLD) with hepatocellular carcinoma (HCC) in the United States from 2004 to 2009, Hepatology 62 (2015) 1723–1730.